Spore-Displayed Enzyme Cascade with Tunable Stoichiometry

Long Chen
Dept. of Chemical and Environmental Engineering, University of California, Riverside, CA 92521

Ashok Mulchandani
Dept. of Chemical and Environmental Engineering, University of California, Riverside, CA 92521

Xin Ge
Dept. of Chemical and Environmental Engineering, University of California, Riverside, CA 92521

DOI 10.1002/btpr.2416
Published online January 28, 2017 in Wiley Online Library (wileyonlinelibrary.com)

Taking the advantages of inert and stable nature of endospores, we developed a biocatalysis platform for multiple enzyme immobilization on Bacillus subtilis spore surface. Among B. subtilis outer coat proteins, CotG mediated a high expression level of Clostridium thermocellum cohesin (CtCoh) with a functional display capability of ~10^4 molecules per spore of xylose reductase-C. thermocellum dockerin fusion protein (XR-CtDoc). By co-immobilization of phosphite dehydrogenase (PTDH) on spore surface via Ruminococcus flavefaciens cohesin-dockerin modules, regeneration of NADPH was achieved. Both xylose reductase (XR) and PTDH exhibited enhanced stability upon spore surface display. More importantly, by altering the copy numbers of CtCoh and RfCoh fused with CotG, the molar ratio between immobilized enzymes was adjusted in a controllable manner. Optimization of spore-displayed XR/PTDH stoichiometry resulted in increased yields of xylitol. In conclusion, endospore surface display presents a novel approach for enzyme cascade immobilization with improved stability and tunable stoichiometry.
 Biotechnol. Prog., 33:383–389, 2017
Keywords: spore surface display, enzyme immobilization, enzyme cascade, cofactor regeneration, cohesin-dockerin interaction

Introduction

Enzymes catalyze specific reactions at environmentally benign conditions and often generate chiral products, therefore holding great promises for a broad range of chemical conversions.[1,2] However, employing enzymes for large-scale industrial applications is in general limited by the high cost of protein purification and the low stability of biocatalysts. Using whole cells that carry the enzymes of interest can avoid purification, but cell membrane and cell wall barriers restrain substrate and product transports. In addition, native metabolisms of the host cells often interfere with the target reactions, generating byproducts or even adverse cellular effects. To overcome these issues, display of enzymes on microbial cell surfaces have been developed especially for bacteria and yeasts.[3–7] Taking the advantages of stable and inert nature of endospores, this study aims to develop a platform technology of biocatalysis based on *Bacillus subtilis* endospore surface display. When starved or under extreme conditions, *e.g.* temperatures, radiation, pH, and harmful chemical agents, *B. subtilis* cells undergo asymmetrical division to form two compartments called mother cell and forespore.[8] During sporulation, mother cell engulfs forespore, then a variety of cortex and coat proteins are produced in the mother cell cytoplasm and assembled on surface of the nascent spore. Finally, mother cells lysate and matured spores are released. Because coat protein expression and localization on endospore surface do not require protein transportation across cell membrane,[9,10] this approach provides an attractive strategy to display complex multimeric enzymes and enzyme cascades, which can be challenging for conventional microbial display techniques.[11]

Pioneer studies of spore surface display have mainly focused on the development of robust vaccine delivery methods,[12–15] or establishing display systems using model proteins such as green fluorescent protein and streptavidin.[16,17] Adsorption of multimeric β-galactosidase on wild type and mutated *B. subtilis* spores have been reported, and the results suggested dramatic improvements of enzyme stability at acidic pHs and high temperatures.[18] However, adsorption capacity via the passive and nonspecific interactions likely depends on the properties of target enzymes. Since several coat proteins of spore outer surface have been identified (*e.g.* CotB, CotC, CotG, and OxdD),[19,20] they were employed as fusion partners to display heterologous proteins,[21–23] but display of enzyme cascades has not been reported. Herein we study spore surface display of multiple enzymes in a stoichiometrically controllable manner by recruiting cohesin (Coh) and dockerin (Doc) modules derived from cellulosomes (Figure 1).[24,25]

Additional Supporting Information may be found in the online version of this article.

Correspondence concerning this article should be addressed to: Xin Ge at xge@engr.ucr.edu.

Materials and Methods

Construction of spore surface display plasmids and transformation of *B. Subtilis*

Clostridium thermocellum (ATCC# 27405) type I cohesin gene (CtCoh) was amplified using polymerase chain reactions (PCRs) from genomic DNA with a C-terminal FLAG tag, and cloned into a *Bacillus* chromosome integration vector pDG364 to yield pDG364-CtCoh. The genes encoding spore coat proteins CotB, CotC, and CotG including their promoter regions were amplified from *B. subtilis* PY79 genome and cloned into pDG364-CtCoh, resulting in pDG364-CotX-CtCoh (CotX = CotB/C/G) (Figure 2A). One, two or three repeats of *Ruminococcus flavefaciens* type I cohesin (RfCoh) genes were PCR amplified from pET20b-cbm-scaf3[26] and cloned into pDG364-CotG-CtCoh, to give pDG364-Scaf11, pDG364-Scaf12, and pDG364-Scaf13, respectively (Figure 3A). All constructed plasmids were confirmed by restriction enzyme mapping and DNA sequencing. For chromosomal integration at α-amylase locus, the constructs were linearized by *Xho*I digestion and transformed into *B. subtilis* competent cells.[27] Transformants were selected on agar plates supplemented with 5 μg mL^{-1} chloramphenicol.

Cloning, expression and purification of XR-CtDoc and PTDH-RfDoc

The gene encoding a *C. thermocellum* type I dockerin (CtDoc) was PCR amplified with a C-terminal c-Myc tag, and cloned into pET28b(+) to give pET28b-CtDoc. *Neurospora crassa* D-xylose reductase (XR) gene was amplified from pTrcXR[28] and inserted into pET28b-CtDoc, resulting in pET28b-XR-CtDoc. Similarly, genes of *Pseudomonas stutzeri* WM88 phosphite dehydrogenase (PTDH)[29] and *Ruminococcus flavefaciens* type I dockrin (RfDoc)[26] with a C-terminal c-Myc tag were PCR amplified and cloned to generate pET28b-PTDH-RfDoc. Constructed plasmids were confirmed by DNA sequencing and transformed into *E. coli* BL21(DE3) for production of XR-CtDoc and PTDH-RfDoc. When OD_{600} reached 0.8, 0.4 mM IPTG was added to induce protein expression at room temperature overnight. Both XR-CtDoc and PTDH-RfDoc were purified with Ni-NTA agarose via their N-terminal 6 × His tags. Concentrations of purified proteins were determined using a BioTek spectrophotometer with calculated extinction coefficients ε_{280} = 63,830 M^{-1} cm^{-1} and 33,460 M^{-1} cm^{-1} for XR-CtDoc and PTDH-RfDoc, respectively.

Spore production and coat protein extraction

Bacillus subtilis cells were cultured in 2 × SG medium at 37°C for 24–28 h,[8] and the optimal culture time for spore harvest was determined by OD measurements and microscopic imaging (Figure S1). Spores were collected by centrifugation at 4,000*g* for 6 min and washed with 1.5 M KCl and 0.5 M NaCl. Unsporulated mother cells were lysed by incubation with 50 μg mL^{-1} egg white lysozyme (Sigma-Aldrich) in 50 mM Tris-HCl (pH 7.2) at 37°C for 1 h, and spores were separated from cell debris by centrifugation. Obtained spores were then washed with 1 M NaCl, water, 0.05% sodium dodecyl sulfate (SDS) and water, and finally resuspended in 50 mM phosphate buffer (pH 7.0). For immunofluorescence microscopy, 5 OD spores sampled at different culture times were washed four times with 50 mM Tris-HCl (pH7.5) 150 mM NaCl and incubated with 1 μL anti-FLAG-FITC

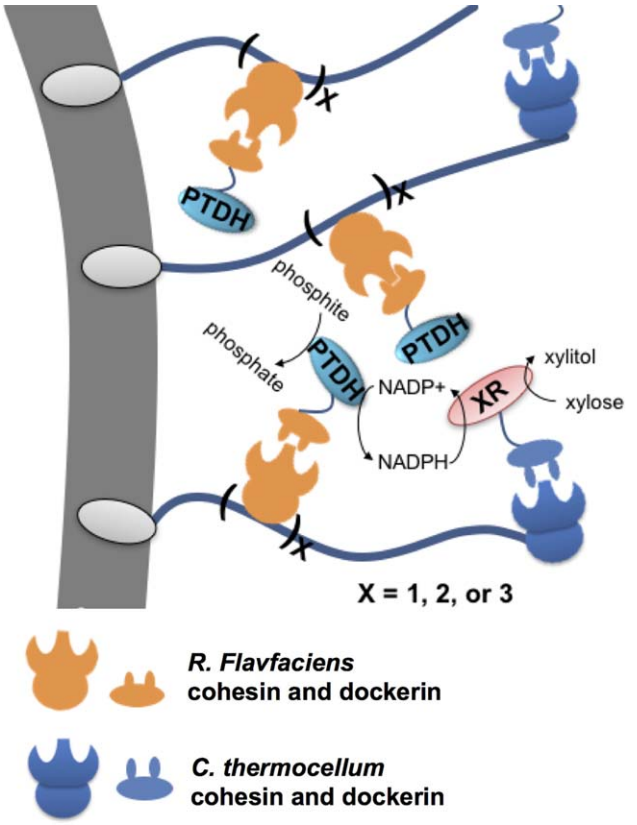

Figure 1. Simultaneously co-immobilizing multiple enzymes on endospore surface with controllable stoichiometry.

(Sigma-Aldrich) for 30 min under gentle rotation. After washing, spore samples were imaged by an Olympus immunofluorescence microscope. For biocatalysis assays, excess amounts of purified dockerin-fused enzymes were mixed with prepared spore suspension for 5 min, then washed with phosphate buffer twice to remove nonspecifically bound proteins. Alternatively, cell lysates containing enzyme-dockerin fusion proteins were incubated with cohesin displaying spores for direct enzyme immobilization without protein purification.

To release coat proteins and immobilized enzymes for analysis, spores were incubated with 1% SDS and 50 mM dithiothreitol (DTT) at 70°C for 30 min, and centrifuged at 10,000*g* for 10 min. The supernatants were loaded for sodium dodecyl sulfate-polyacrylamide gel electrophoresis (SDS-PAGE) and Western blotting signals were developed using anti-FLAG-HRP (Bethyl Laboratories) or anti-c-Myc-HRP (Santa Cruz Biotechnology) with supplement of chemiluminescent substrates (Thermo Scientific). The densitometry data of blotting bands were obtained using Image Lab software. For dot blotting, extracted XR-CtDoc/PTDH-RfDoc samples were serially diluted and immobilized on polyvinylidene difluoride membranes. The signals were developed using anti-c-Myc-HRP and chemiluminescent substrates. Quantitative analysis were made by densitometry and compared with purified enzymes as the standards.

Enzymatic reaction assays

Enzyme activities were measured in 50 mM phosphate (pH 7.0, suitable for both enzymes), 0.2 mM NADP(H), 0–200 mM D-xylose or 0–10 mM phosphite. The rates of NADPH consumption (for XR-CtDoc) or generation (for PTDH-RfDoc)

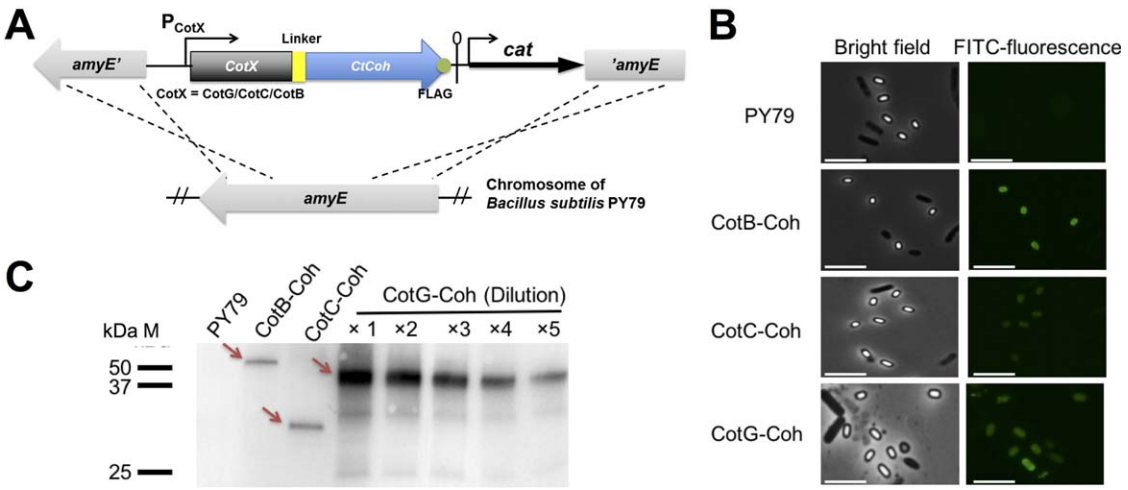

Figure 2. Spore surface display via cohesin-dockerin interaction.

(A) Construction of gene cassettes for display of coat protein-cohesin (CotX-Coh, CotX = CotB/C/G) by chromosomal integration. Purified spores were (B) labeled with anti-FLAG-FITC and examined with fluorescent microscopy, or (C) treated with SDS-DTT solution and examined by Western blotting using anti-FLAG-HRP.

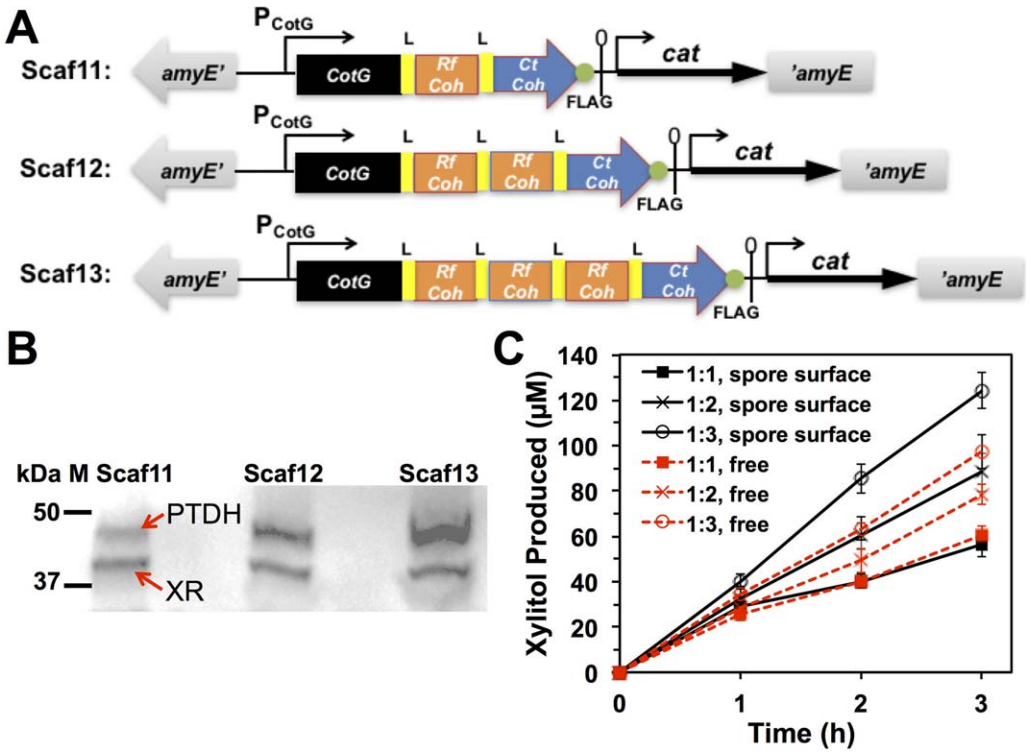

Figure 3. Varying ratios of XR/PTDH on spore surface.

(A) Constructions of scaffold proteins Scaf11 (CtCoh/RfCoh = 1:1), Scaf12 (CtCoh/RfCoh = 1:2), and Scaf13 (CtCoh/RfCoh = 1:3) for chromosomal integration. (B) Analysis of XR-CtDoc and PTDH-RfDoc immobilized on spores. Spores displaying scaffoldins were harvested and incubated with excess amounts of XR-CtDoc and PTDH-RfDoc. After extensive washing, immobilized enzymes were eluted from spores by SDS-DTT for Western blotting. Quantitative densitometry data were analyzed using Image Lab software, and Western blotting experiments were duplicated to obtain the means and S.D. values. (C) Xylitol production via NADPH regeneration and yield improvement by stoichiometry optimization. Assays were performed with XR-CtDoc and PTDH-RfDoc either immobilized on spores (black) or in solution (red), in the presence of phosphite, D-xylose, and $NADP^+$. Produced xylitol was quantified with HPLC. Means and S.D. were calculated based on triplicated tests.

were monitored by UV spectrometry at 340 nm (ε = 6,300 M^{-1} cm^{-1}). When both enzymes were present, 5 mM phosphite, 200 mM D-xylose, and 2 mM $NADP^+$ was added to solution or spore suspension. Produced xylitol was quantified by an Agilent HPLC, equipped with an Aminex HPX-87H ion exchange column and a refractive index detector. 5 mM H_2SO_4 was employed as the mobile phase. Experiments were triplicated to obtain the associated means and S.D. values. To estimate capacities of spore surface immobilization, excess XR-CtDoc was incubated with spores displaying CotG-CtCoh, and after washing to remove unbound enzymes, activities of spore suspension were measured. The quantities of enzyme

molecules per spore were calculated based on k_{cat} of XR-CtDoc and the correlation between spore numbers and optical density at 600 nm (OD_{600}), *i.e.* 1.5×10^8 CFU mL^{-1} at one unit of OD_{600}.

Results

CotG mediated high display levels of scaffoldins

Within the > 50 polypeptides involved in coat assembly, the major components of the outer coat (the most outside layer of endospores) and their associated genes have been identified by biochemical and genomic means.[19,20] Since these discoveries, several proteins have been displayed on the surface of spores by fusing the target proteins to the C-terminus of one of the major outer coat proteins such as CotB, CotC, CotG, and OxdD.[21–23] Different from all previous spore display studies, we intended to immobilize multiple enzymes with controllable stoichiometry. We hypothesized that using the dockerin and cohesin modules derived from cellulosomes can achieve this goal.[24,25] To identify the most suitable *B. subtilis* coat proteins for enzyme immobilization via cohesin-dockerin, *C. thermocellum* type I cohesin (CtCoh) was cloned to the C-termini of CotB/CotC/CotG, which were regulated by their native promoters (Figure 2A). In addition, a FLAG tag was introduced at the C-termini of CotX-CtCoh for detection. After chromosome integration, spores carrying CotX-CtCoh were harvested at 24 h, which was the optimal culture time for sporulation (Figure S1). Collected spores were then labeled with anti-FLAG-FITC and analyzed by fluorescence microscopy. As shown in Figure 2B, the spores obtained from CotB/C/G-CtCoh strains all exhibited strong fluorescence, whereas PY79 host without transformation did not show detectable signals, indicating successful display of scaffoldins on spore surface. More specifically, CotB and CotG fusions exhibited higher fluorescence signals than CotC. Furthermore, the outer coat fractions were extracted from spores by SDS-DTT treatment to visualize the expression levels of cohesins by Western blotting. The results showed single bands with expected MWs for CotB-CtCoh (50 kDa), CotC-CtCoh (33 kDa), and CotG-CtCoh (43 kDa) (Figure 1C). It also suggested that CotG-CtCoh was expressed at least 5-fold more than CotB/C-CtCoh.

Xylose reductase immobilization via cohesin-dockerin interaction

Enzymatic redox reactions catalyzed by dehydrogenases and reductases are widely applied for the synthesis of specialty chemicals, such as single-isomer alcohols, chiral amino acids, and other enantiomeric pure compounds.[30,31] Among ketoreductases, xylose reductase (XR, EC1.1.1.307) has gained interests not only because the native reaction it catalyzes, xylose to xylitol, is the first step to utilize C5 for biofuel production, but also it accepts many non-natural substrates for chiral conversions.[32] Particularly, XR from xylose assimilating fungus *Neurospora crassa* can utilize both NADH and NADPH and catalyzes reduction of a variety of sugar substrates over a wide pH range.[33] To display *N. crassa* XR on spore surface via anchored scaffoldins, its gene was cloned to the N-terminus of *C. thermocellum* type I dockerin (CtDoc), and XR-CtDoc fusion protein was heterologously expressed in *E. coli*. Cell lysate containing XR-CtDoc was then incubated with the suspension of prepared scaffoldin-displaying spores allowing self-assembly governed by cohesin-dockerin interaction. After washes to remove nonspecifically bound enzymes, the resulted spores were tested for XR activity. Because of the long and flexible linkers between coat protein and cohesin and between XR and dockerin, it is expected that XR immobilized on the spore surface has a similar specific activity as that of free XR. Results indicated that spores displaying XR-CtDoc via CotG-CtCoh exhibited a rapid NADPH consumption, at a rate of 22 ± 1.8 μM min^{-1} per OD spores. Given that an OD_{600} is equivalent to 1.5×10^8 spores mL^{-1} and the measured turnover rate of XR was 42 s^{-1} at pH7.0, the display capacity was estimated to be $\sim 10^4$ XR-CtDoc molecules per spore carrying CotG-CtCoh.

Xylitol production by multiple enzyme display

Most oxidoreductases involved in specialty chemical synthesis, including XR, utilize pyridine nucleotides, $NAD(P)^+$ and NAD(P)H, as cofactors for catalysis. Because these cofactors are extremely expensive ($\sim$\$1000 $mole^{-1}$) and are consumed in stoichiometric quantity, their recycling is essential for the *in vitro* reactions to be cost-effective. Furthermore, cofactor regeneration also helps drive the thermodynamically unfavorable reaction toward product formation and thereby improves the overall yields.[34–36] We therefore further investigated the feasibility of simultaneously immobilizing a second enzyme on spore surface for NAD(P)H regeneration. Phosphite dehydrogenase (PTDH) catalyzes the conversion of phosphite to phosphate, which is coupled with reduction of $NADP^+$ to NADPH.[37] Because this irreversible reaction utilizes an inexpensive inorganic compound as its co-substrate, PTDH has been recognized as an ideal enzyme for cofactor regeneration.[38] However, PTDH exhibited a relatively low specific activity with a measured turnover rate of 2.3 s^{-1} when $NADP^+$ was used as the cofactor. Inspired by the substrate channeling phenomena seen in natural and synthetic multi-enzyme cascades, we aimed to improve the efficiency of cofactor regeneration not by engineering of PTDH itself but by providing a close proximity with XR for an efficient NADPH–$NADP^+$ recycling through their spatial organization on the surface of spores.

To independently control the numbers of PTDH and XR immobilized on spores, *Ruminococcus flavefaciens* type I cohesin-dockerin modules were utilized for recruitment of *Pseudomonas stutzeri* PTDH. PTDH gene was cloned to the N-terminus of *R. flavefaciens* dockerin (RfDoc), and PTDH-RfDoc chimeric protein was produced in *E. coli*. *R. flavefaciens* cohesin (RfCoh) was cloned between CotG and CtCoh on the *B. subtilis* chromosomal integration plasmid, to encode a tripartite fusion protein CotG-RfCoh-CtCoh (Figure 3A). For detection, a c-Myc tag was incorporated at the C-terminus of PTDH-RfDoc. Similar to XR-displaying spores, the spores carrying XR and PTDH were tested by Western blotting with anti-c-Myc-HRP. Results indicated that both enzymes were present in the spore coat extraction samples with a molar ratio of PTDH:XR = 0.7 ± 0.02 (given by duplicated western blotting experiments) (Figure 3B). The spores displaying both enzymes were then subjected to catalysis assays with substrates D-xylose and phosphite. Because the cofactor was provided at its oxidized form as $NADP^+$, xylitol can only be produced when both enzymes are functional. After $\sim$16 h reaction, 77.2 ± 8.6 μM xylitol was produced per OD spores, with an initial rate of 18.0 ± 2.6 μM xylitol produced per OD spores per hour (Figure 3C). Using the same amounts of enzymes, catalysis assays were also performed in solutions to compare their specific activities. The results suggested that the

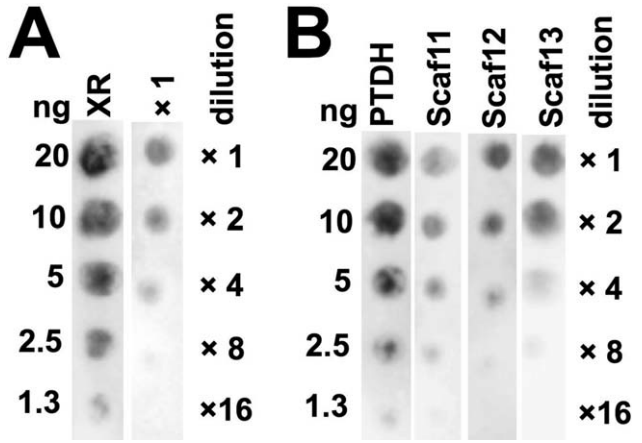

Figure 4. Quantification of immobilized (A) XR-CtDoc and (B) PTDH-RfDoc by dot blotting.

10 OD spores displaying scaffoldins were harvested and incubated with excess amounts of XR-CtDoc or PTDH-RfDoc. After washing, immobilized enzymes were eluted by SDS-DTT and serially diluted for dot blotting analysis. Purified enzymes were used as the standards.

enhancement by spore display is negligible, presumably because the spatial distance between XR and PTDH on spores via the scaffodin containing one CtCoh and one RfCoh, was not proximal enough to drive significant substrate channeling.

Improved product yields by controlling enzyme stoichiometry

It is not uncommon that the kinetics of coupled enzymes in either natural or artificial metabolic cascades are not in balance. This imbalance usually results in the accumulation of intermediates and/or sub-optimal product yields. Optimizing the ratios of enzymes within a cascade reaction is a practical strategy to improve the rate of overall conversion. To achieve tunable stoichiometry, the ratio between XR and PTDH was manipulated by altering the copy numbers of the associated cohesins on the anchoring scaffoldins (Figure 3A). Since PTDH has a significantly lower specific activity than that of XR at the tested conditions, higher copy numbers for PTDH is desirable. Two more scaffoldin structures were constructed by inserting either one or two more RfCoh domains at the N-terminus of CtCoh in the previously constructed CotG-RfCoh-CtCoh expression cassette, generating additional XR/PTDH stoichiometry of 1:2 and 1:3, respectively. The DNA fragments encoding these multi-cohesin fusions were prepared by overlapping-extension PCRs, and the resulting constructs were nominated as Scaf11, Scaf12, and Scaf13 reflecting there were one CtCoh domain and one, two or three RfCoh domain(s) per scaffoldin molecule. As abovementioned, display of Scaf11, Scaf12, and Scaf13 on the spore surface were achieved by cell culture in sporulation-inducing media 2 × SG for 24 h. The spores carrying various scaffoldins were directly incubated with lysates of cells expressing XR-CtDoc and PTDH-RfDoc to assemble multi-enzyme complexes on spore surface. The compositions of these obtained enzyme complexes were biochemically characterized by coat protein extraction and Western blotting. Results confirmed that increased amounts of PTDH were incorporated into the spore-displayed complexes when more RfCoh modules were utilized, while the amounts of XR remained relatively unchanged (Figure 3B). Quantitative analysis of western blotting bands suggested that the ratios of PTDH-RfDoc:XR-CtDoc were 1.6 ± 0.3 and 2.9 ± 0.3 for Scaff12 and Scaf13, respectively (the means and S.D. were obtained from duplicated experiments), following the same trend as designs. In enzymatic assays supplied with D-xylose, phosphite, and $NADP^+$, spores carrying Scaf12 and Scaf13 produced $57 \pm 15\%$ and 1.2 ± 0.1 folds more xylitol compared to that of Scaf11. In addition, their initial specific activities were 29.3 ± 0.8 (for Scaf12) and 41.8 ± 0.9 (for Scaf13) $\mu M\ h^{-1}$. In comparison with the activities of the same amounts of enzymes in solutions, the enhancements of spore surface display were approximately 10% for Scaf12 and 30% for Scaf13 (Figure 3C).

To further quantify the capacity and stoichiometry of enzyme immobilization, coat protein extraction samples were subjected to dot blotting and obtained images were quantitatively analyzed for comparison with serially diluted purified enzymes as the standards (Figure 4). Results indicated that the display capacity of XR-CtDoc was 1.5×10^4 molecules per spore, in good agreement with the estimation by catalytic assays. When PTDH-RfDoc was co-displayed, the enzyme amounts were determined as 1.4, 2.5, and 3.6×10^4 molecules per spore for Scaf11, Scaf12, and Scaf13, respectively. Collectively, these results suggested that the molar ratios of XR:PTDH were altered on spore surface as designs and manipulating enzyme stoichiometry resulted in improved product yields.

Spore surface immobilization enhanced enzymes stability

Since the XR and PTDH used in this study showed relatively low stability in solutions,[29,33] we next tested the effects of spore surface immobilization on stability improvement, a phenomenon observed in previous studies.[11,18] After incubation at 25°C for 0–10 h, remaining activities of XR and PTDH in solution or on spore surface were measured. The half-lives of free and spore surface immobilized XR-CtDoc were calculated to be 3.6 and 11.6 h (Figure 5). After 10 h of incubation, immobilized XR-CtDoc still had 45% activity left, while free XR-CtDoc only retained 16% of its activity. A similar stability improvement was observed for PTDH-RfDoc as well. After incubation for 10 h, immobilization helped increase PTDH residual activity from 10 to 24%.

Discussion

As an extreme survival strategy, certain Gram-positive bacteria such as *B. subtilis* undergo a series of developmental processes to form endospores when starved or under adverse conditions. *B. subtilis* sporulation involves more than 120 gene expressions and is associated with several morphological stages: asymmetric cell division, engulfment, cortex and coat assembly, and eventually formation of the matured spore for future germination upon appropriate evironements.[8] To generate reliable enzyme immobilization, sporulation process of *B. subtilis* was monitored by OD_{600} measurements and microscopic imaging the samples before and after lysozyme treatment. Results confirmed that in 2 × SG media, sporulation started as forespore formation at the 12th hour, and mature endospores dominated at the 24th hour, which was the optimal time to harvest *B. subtilis* spores (Figure S1).

Most previous studies of protein immobilization on spore surface utilized one of the following two strategies: passive adsorption[9,18] or direct fusion with a coat protein.[20–23] The amounts of proteins that can be immobilized by these methods

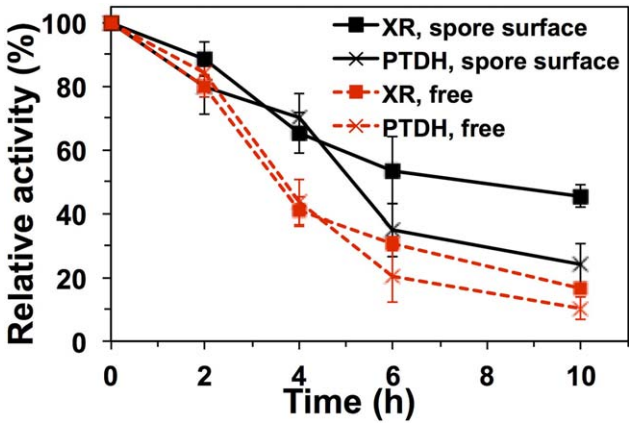

Figure 5. Stability enhancement for enzymes immobilized on spores.

After incubation at 25°C for the indicated periods of time, the relative activities of XR-CtDoc and PTDH-RfDoc on spore surface (black) or in solution (red) were tested. Values represent means and S.D. obtained from triplicated experiments.

primarily depend on the properties of target proteins including charge, size, and hydrophobicity, and thus likely varied for different target enzymes. Here, we developed a general method of spore surface immobilization by employing the strong and specific interaction between cohesin and dockerin derived from cellulosomes of thermophilic bacteria. This approach is presumably less dependent on properties of immobilized enzymes due to the long and flexible linkers between anchoring modules, and therefore is suitable for a broad range of enzymes for biocatalysis applications. Via Coh-Doc, the amount of enzymes displayed on spore surface, $\sim 10^4$ per spore, was significantly higher than direct coat protein-enzyme fusion approach,[21,22] likely because the cohesin-dockerin modules acted as a spacer to extend enzymes away from the spore surface thereby reducing steric hindrance and making enzymes more accessible to their substrates. Display capacities of $2 \times 10^4 - 10^5$ recombinant proteins per *E. coli* cell have been reported with its Lpp-OmpA hybrid or autodisplay systems.[39,40] And for *Saccharomyces cerevisiae*, $10^4 - 10^5$ heterologous proteins were displayed per cell.[41] Therefore, the display density on spores is less than that of *E. coli*, but roughly equivalent to that of baker's yeast for per unit of surface area, considering that the diameter of yeast cells is a few times larger than that of *B. subtilis* spores.

After verifying the functions of XR and PTDH individually on spore surface, we further coupled the two enzymes on spores for enzymatic assays with the presence of merely xylose, phosphite, and $NADP^+$. The regeneration of cofactor and the production of xylitol confirmed the simultaneous displays of both XR and PTDH in their functional formats on spore surface. It is worth to mention that the cascade reaction was performed at pH 7.0 in this study, which is not the optimal pH for either enzymes (pH 5.5 for XR and pH 8.0 for PTDH) but retains >50% activities for both enzymes.

Fine-tuning enzyme ratios is difficult to achieve in whole-cell biocatalysts, because protein expression is a multi-step process, in which the transcript amounts, mRNA stability, translation rate, and folding speed and efficiency of produced polypeptides all contribute to catalytic activities. Free enzyme complexes are able to regulate enzyme ratios but suffer from low stability and high purification costs. Coupling the spore display and specific Coh-Doc interaction, this study addresses these problems by developing a designer biocatalyst system that facilitates the manipulation of enzyme stoichiometry. We demonstrated that the ratio of enzymes, *i.e.* XR/PTDH in this current study, could be adjusted through recruiting different copy numbers of their associated cohesin modules on spore surface. More importantly, it showed that with higher ratios of PTDH over XR, the yields of xylitol were significantly increased.

Another advantage of enzyme immobilization on spores is stability enhancement. Our results proved that by displaying on spore surface, retained activities of XR and PTDH were dramatically improved 2.8-fold and 2.3-fold, respectively after 10 h of incubation at 25°C (Figure 5). The spore surface, like many other solid supports, presumably prevents protein denaturation.[42,43] This stability improvement could be particularly beneficial when biocatalysis is performed in organic solvents.[11,44]

In summary, via cohesin-dockerin interaction, two enzymes were immobilized on *B. subtilis* endospore surface in a stoichiometrically controllable manner. Functional co-immobilization of both XR and PTDH resulted in cofactor regeneration and production of xylitol. With increasing amounts of PTDH on spore surface by manipulating the copy numbers of the associated cohesins, a higher product generation rate was achieved. One future development could be the co-expression of both scaffoldins and enzymes in the mother cell compartment for self-assembly during sporulation process.

Acknowledgments

This study was supported by National Science Foundation (CBET 1265044). We appreciate the *Bacillus* Genetics Stock Center providing plasmid pDG364 and strain PY79. We would like to thank Professors Wilfred A. von der Donk and Huimin Zhao of UIUC for sharing XR and PTDH genes, and Professor Percival Zhang of Virginia Tech for cohesin and dockerin genes.

Literature Cited

1. Bommarius AS. Biocatalysis: a status report. *Annu Rev Chem Biomol Eng*. 2015;6:319–345.
2. Choi JM, Han SS, Kim HS. Industrial applications of enzyme biocatalysis: current status and future aspects. *Biotechnol Adv*. 2015;33:1443–1454.
3. Schüürmann J, Quehl P, Festel G, Jose J. Bacterial whole-cell biocatalysts by surface display of enzymes: toward industrial application. *Appl Microbiol Biotechnol*. 2014;98:8031–8046.
4. Tanaka T, Kondo A. Cell-surface display of enzymes by the yeast Saccharomyces cerevisiae for synthetic biology. *FEMS Yeast Res*. 2015;15:1–9.
5. Tozakidis IE, Sichwart S, Jose J. Going beyond *E. coli*: autotransporter based surface display on alternative host organisms. *New Biotechnol*. 2015;32:644–650.
6. Smith MR, Khera E, Wen F. Engineering novel and improved biocatalysts by cell surface display. *Ind Eng Chem Res*. 2015; 54:4021–4032.
7. Liu Y, Zhang R, Lian Z, Wang S, Wright AT. Yeast cell surface display for lipase whole cell catalyst and its applications. *J Mol Catalysis B Enzymatic*. 2014;106:17–25.
8. Cutting SM, Vander Horn PB. Sporulation, germination, and outgrowth. In: Harwood CR, Cutting SM, editors. *Molecular Biological Methods for Bacillus*. Chichester, United Kingdom: John Wiley & Sons, Ltd.; 1990:391–450.
9. Pan JG, Choi SK, Jung HC, Kim EJ. Display of native proteins on *Bacillus subtilis* spores. *FEMS Microbiol Lett*. 2014;358: 209–217.

10. Kim J, Schumann W. Display of proteins on *Bacillus subtilis* endospores. *Cell Mol Life Sci*. 2009;66:3127–3136.
11. Kwon SJ, Jung HC, Pan JG. Transgalactosylation in a water-solvent biphasic reaction system with β-galactosidase displayed on the surfaces of bacillus subtilis spores. *Appl Environ Microbiol*. 2007;73:2251–2256.
12. Knecht LD, Pasini P, Daunert S. Bacterial spores as platforms for bioanalytical and biomedical applications. *Anal Bioanal Chem*. 2011;400:977–989.
13. Duc le H, Hong HA, Fairweather N, Ricca E, Cutting SM. Bacterial spores as vaccine vehicles. *Infect Immun*. 2003;71: 2810–2818.
14. Duc le H, Hong HA, Atkins HS, Flick-Smith HC, Durrani Z, Rijpkema S, Titball RW, Cutting SM. Immunization against anthrax using *Bacillus subtilis* spores expressing the anthrax protective antigen. *Vaccine* 2007;25:346–355.
15. Cutting SM, Hong HA, Baccigalupi L, Ricca E. Oral vaccine delivery by recombinant spore probiotics. *Int Rev Immunol*. 2009;28:487–505.
16. Kim JH, Lee CS, Kim BG. Spore-displayed streptavidin: a live diagnostic tool in biotechnology. *Biochem Biophys Res Commun*. 2005;331:210–214.
17. Kim JH, Roh C, Lee CW, Kyung D, Choi SK, Jung HC, Pan JG, Kim BG. Bacterial surface display of GFP(uv) on *Bacillus subtilis* spores. *J Microbiol Biotechnol*. 2007;17:677–680.
18. Sirec T, Strazzulli A, Isticato R, De Felice M, Moracci M, Ricca E. Adsorption of β-galactosidase of *Alicyclobacillus acidocaldarius* on wild type and mutants spores of *Bacillus subtilis*. *Microb Cell Fact*. 2012;11:100.
19. Donovan W, Zheng LB, Sandman K, Losick R. Genes encoding spore coat polypeptides from *Bacillus subtilis*. *J Mol Biol*. 1987; 196:1–10.
20. Driks A. *Bacillus subtilis* spore coat. *Microbiol Mol Biol Rev*. 1999;63:1–20.
21. Isticato R, Cangiano G, Tran HT, Ciabattini A, Medaglini D, Oggioni MR, De Felice M, Pozzi G, Ricca E. Surface display of recombinant proteins on *Bacillus subtilis* spores. *J Bacteriol*. 2001;183:6294–6301.
22. Isticato R, Di Mase DS, Mauriello EM, De Felice M, Ricca E. Amino terminal fusion of heterologous proteins to CotC increases display efficiencies in the *Bacillus subtilis* spore system. *Biotechniques* 2007;42:151–156.
23. Costa T, Steil L, Martins LO, Völker U, Henriques AO. Assembly of an oxalate decarboxylase produced under σ^K control into the Bacillus subtilis spore coat. *J Bacteriol*. 2004; 186:1462–1474.
24. Doi RH, Kosugi A. Cellulosomes: plant-cell-wall-degrading enzyme complexes. *Nature Rev Microbiol*. 2004;2:541–551.
25. Bayer EA, Belaich JP, Shoham Y, Lamed R. The cellulosomes: multienzyme machines for degradation of plant cell wall polysaccharides. *Annu Rev Microbiol*. 2004;58:521–554.
26. You C, Zhang YHP. Annexation of a high-activity enzyme in a synthetic three-enzyme complex greatly decreases the degree of substrate channeling. *ACS Synth Biol*. 2014;3:380–386.
27. Zhang XZ, You C, Zhang YHP. Transformation of Bacillus subtilis. *Methods Mol Biol*. 2014:1151:95–101.
28. Nair NU, Zhao H. Selective reduction of xylose to xylitol from a mixture of hemicellulosic sugars. *Metab Eng*. 2010;12:462–468.
29. Costas AMG, White AK, Metcalf WW. Purification and characterization of a novel phosphorus-oxidizing enzyme from *Pseudomonas stutzeri* WM88. *J Biol Chem*. 2001;276:17429–17436.
30. Musa MM, Phillips RS. Recent advances in alcohol dehydrogenase-catalyzed asymmetric production of hydrophobic alcohols. *Catal Sci Technol*. 2011;1:1311–1323.
31. Chen Y, Chen C, Wu X. Dicarbonyl reduction by single enzyme for preparation of chiral diols. *Chem Soc Rev*. 2012;41:1742–1753.
32. Kratzer R, Nidetzky B. Identification of *Candida tenuis* xylose reductase as highly selective biocatalyst for the synthesis of aromatic alpha-hydroxy esters and improvement of its efficiency by protein engineering. *Chem Commun*. 2007;10:1047–1049.
33. Woodyer R, Simurdiak M, van der Donk WA, Zhao H. Heterologous expression, purification, and characterization of a highly active xylose reductase from Neurospora crassa. *Appl Environ Microbiol*. 2005;71:1642–1647.
34. van der Donk WA, Zhao H. Recent developments in pyridine nucleotide regeneration. *Curr Opin Biotechnol*. 2003;14:421–426.
35. Weckbecker A, Groger H, Hummel W. Regeneration of nicotinamide coenzymes: principles and applications for the synthesis of chiral compounds. *Adv Biochem Eng Biotechnol*. 2010;120: 195–242.
36. Abu R, Woodley JM. Application of enzyme coupling reactions to shift thermodynamically limited biocatalytic reactions. *ChemCatChem*. 2015;7:3094–3105.
37. Relyea HA, van der Donk WA. Mechanism and applications of phosphite dehydrogenase. *Bioorg Chem*. 2005;33:171–189.
38. Johannes TW, Woodyer RD, Zhao H. Efficient regeneration of NADPH using an engineered phosphite dehydrogenase. *Biotechnol Bioeng*. 2007;96:18–26.
39. Francisco JA, Campbell R, Iverson BL, Georgiou G. Production and fluorescence-activated cell sorting of Escherichia coli expressing a functional antibody fragment on the external surface. *Proc Natl Acad Sci USA*. 1993;90:10444–10448.
40. Jose J, Meyer TF. The autodisplay story, from discovery to biotechnical and biomedical applications. *Microbiol Mol Biol Rev*. 2007;71:600–619.
41. Pepper LR, Cho YK, Boder ET, Shusta EV. A decade of yeast surface display technology: where are we now? *Comb Chem High Throughput Screen*. 2008;11:127–134.
42. Wang N, Chang C, Yao Q, Li G, Qin L, Chen L, Chen K. Display of *Bombyx mori* alcohol dehydrogenases on the *Bacillus subtilis* spore surface to enhance enzymatic activity under adverse conditions. *PLoS ONE*. 2011;6:e21454.
43. Yim SK, Jung HC, Yun CH, Pan JG. Functional expression in *Bacillus subtilis* of mammalian NADPH-cytochrome P450 oxidoreductase and its spore-display. *Protein Expr Purif*. 2009;63:5–11.
44. Jia H, Lee FS, Farinas ET. Bacillus subtilis spore display of laccase for evolution under extreme conditions of high concentrations of organic solvent. *ACS Comb Sci*. 2014;16:665–669.

Manuscript received Aug. 10, 2016, and revision received Nov. 2, 2016.

Supporting Information

Sporulation Process Optimization. To maximize spore yields for biocatalysis applications, sporulation process of *B. subtilis* strain PY79 was studied by measuring OD_{600} and observing the morphology under a microscope at different time points when cultured in sporulation medium. Collected culture samples were also treated with lysozyme to lyse vegetative cells followed by repeated centrifugation and washes to remove cell debris. Thus, the OD_{600} values of post-lysozyme treatment were associated with formed spores. As expected *B. subtilis* cells quickly grew to OD ~2.5 in 6 hours after inoculation without detectable forespore or spore formation (**Fig S1A)**. Microscope images taken at the 12th hour showed forespores appeared in a small fraction of cells (indicated by arrows in **Fig S1B**), which correlated with a slight increase of OD_{600} associated with spores, while OD_{600} of the cell sample without lysozyme treatment increased to ~3.0. As significant amounts of nutrients were consumed between 12 and 20 hours, OD_{600} associated with spores rapidly increased by 1.8 units, while the OD_{600} of cell samples without lysozyme treatment only increased by 0.9, indicating more vegetative cells developed to spores during the period. At the 20th hour, the culture sample was predominated with mature endospores. After 20 hours, the OD_{600} associated with spores was relatively constant at ~1.8, but the OD_{600} for culture mixture without lysozyme treatment started to decrease at the 26th hour, suggesting cell death.

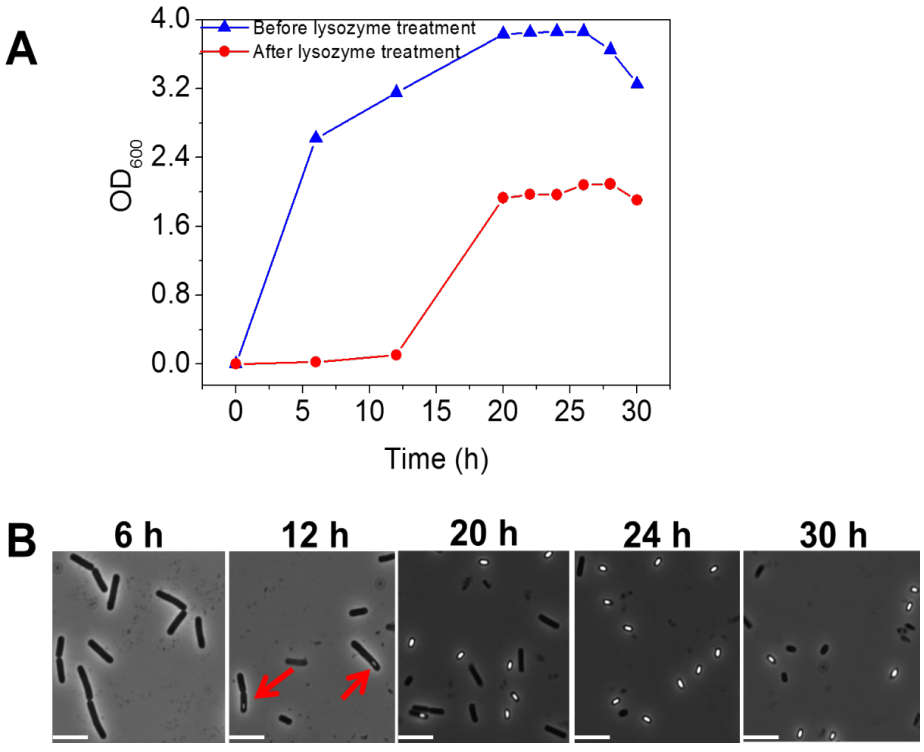

Figure S1. Sporulation process of *B. subtilis*. (A) OD_{600} curves of *B. subtilis* cultured in 2×SG medium before lysozyme treatment (including vegetative cells, spores, and debris of autolysed mother cells) and after lysozyme treatment and wash/centrifugation cycles (associated with spores only). (B) Microscopic images at different culture time. Arrows indicate the appearance of forespores at 12 hour. Mature spores predominated in the 24 hour culture sample. Bars = 5 μm.